Titre: Title:	Effect of freeze-thaw cycles on engineering properties of nano-SiO_2 enhanced microbially induced calcium carbonate precipitation in kaolinite clay
Auteurs: Authors:	Sara Ghalandarzadeh, Benoit Courcelles, Richard Boudreault, Lukas U. Arenson, & Pooneh Maghoul
Date:	2025
Type:	Article de revue / Article
Référence: Citation:	Ghalandarzadeh, S., Courcelles, B., Boudreault, R., Arenson, L. U., & Maghoul, P. (2025). Effect of freeze-thaw cycles on engineering properties of nano-SiO_2 enhanced microbially induced calcium carbonate precipitation in kaolinite clay. Cold Regions Science and Technology, 234, 104459 (14 pages). https://doi.org/10.1016/j.coldregions.2025.104459

Cold Regions Science and Technology 234 (2025) 104459

Contents lists available at ScienceDirect

Cold Regions Science and Technology

journal homepage: www.elsevier.com/locate/coldregions

Effect of freeze-thaw cycles on engineering properties of nano-SiO_2 enhanced microbially induced calcium carbonate precipitation in kaolinite clay

Sara Ghalandarzadeh [a], Benoit Courcelles [a], Richard Boudreault [a], Lukas U. Arenson [b,a], Pooneh Maghoul [a,c,*]

[a] Sustainable Infrastructure and Geoengineering Lab (SIGLab), Department of Civil, Geological and Mining Engineering, Polytechnique Montréal, Montréal, Canada
[b] BGC Engineering Inc, Vancouver, Canada
[c] Sustainable Infrastructure in Cold Regions Lead, United Nations University Institute for Water, Environment and Health (UNU-INWEH), Canada

ARTICLE INFO

Keywords:
MICP
Bacillus pasteurii
Nano-SiO_2
Nature-based soil stabilization
Biocalcification
Kaolinite
Freeze-thaw cycles

ABSTRACT

Microbially Induced Calcium Carbonate Precipitation (MICP) is a nature-based soil stabilization technique, that has substantially lower environmental impacts compared to conventional chemical-based methods. However, its application in fine-grained soils, such as clay, remains challenging due to the soil's plasticity and saturation levels, which can hinder the effectiveness of MICP. Furthermore, the performance of MICP-treated soils under extreme environmental conditions, such as cyclic freeze-thaw (FT) processes common in cold regions, has not been fully explored. This study addresses these challenges by investigating the enhancement of MICP using nano-SiO_2 in kaolinite clay subjected to FT cycles, proposing a novel nano-bio soil stabilization method for cold regions. Samples treated with 30 % bacterial (e.g. *Bacillus Pasteurii*) and cementation solutions, supplemented with 1.5 % nano-SiO_2 over four weeks of curing time, were subjected to cyclic FT and triaxial compression tests. Treated samples demonstrated significantly higher peak shear strengths compared to untreated samples under varying confining stress conditions. A reduction in strength was observed in the treated samples as the number of FT cycles increased. However, by the sixth FT cycle, the treated samples showed a significant improvement in strength compared to the untreated samples, with increases of 4.00, 4.96, and 3.49 times under confining pressures of 50, 100, and 150 kPa, respectively. These findings highlight the effectiveness of the stabilization method under cyclic FT conditions. Microstructural analyses revealed increased calcium carbonate content and altered soil texture in treated samples, which affirms the effectiveness of the nano-bio stabilization approach.

1. Introduction

In cold regions, repetitive freeze-thaw cycles (FTCs) in soils may pose a risk to the integrity of structures due to potential reductions in soil strength. Soil micro- and macrostructures, particularly in frost-susceptible soils, undergo alterations during FTCs, primarily due to the formation and melting of ice pores and ice inclusions in the soil. Various research studies have focused on investigating the influence of FTCs on different physical and mechanical properties of soils. Notably, characteristics such as resilient modulus and unconfined compressive strength (UCS) change significantly as a result of the phase change of pore water during the freeze-thaw process (Qi et al., 2008).

The number of FTCs is a critical parameter that significantly impacts the engineering properties of geomaterials (Viklander and Eigenbrod, 2000). These cycles cause particle rearrangements within the soil, leading to a reduction in its strength. Previous studies have shown that increasing the number of FTCs up to a certain threshold leads to a decline in soil strength. Nonetheless, once this threshold is exceeded, prolonged periods of freeze and thaw have only a negligible influence on the mechanical properties of the soil. This phenomenon is likely attributed to the soil structure eventually attaining a new equilibrium (Wang et al., 2007). Tang et al. (2017) performed a series of triaxial Consolidated-Undrained (CU) tests to evaluate the effect of FTCs on the strength characteristics of expansive soils. It was observed that after only

* Corresponding author at: Sustainable Infrastructure and Geoengineering Lab (SIGLab), Department of Civil, Geological and Mining Engineering, Polytechnique Montréal, Montréal, Canada.
E-mail address: pooneh.maghoul@polymtl.ca (P. Maghoul).

https://doi.org/10.1016/j.coldregions.2025.104459
Received 2 October 2024; Received in revised form 14 February 2025; Accepted 15 February 2025
Available online 21 February 2025

five FTCs, the strength characteristics of an expansive soil remained relatively unchanged. In another study conducted by (Wang et al., 2018), it was observed that as the number of FTCs increases, there is a significant decline in both, the maximum value of the deviatoric stress (defined as static strength) and cohesion of the soil. In contrast, the internal friction angle exhibits an exponential increase until it stabilized at a constant value. Zhang et al. (2022) performed a series of Unconsolidated-Undrained (UU) triaxial tests on a typical clay subjected to different FTCs a closed system to understand the changes in strength parameters. A 6–22 % reduction in the failure strength was observed compared to the initial condition (before FTCs). It was also observed that the stress-strain behavior altered from strain hardening to strain softening by increasing the FTCs. The elastic modulus decreased significantly after the first FTC and the failure strength progressively plummeted as the number of FTCs increased, and eventually tended to remain stable when the FTCs reached 10.

Wu et al. (2023) investigated the effect of FTCs on the strength of volcanic ash through triaxial testing. Samples with varying initial water contents were tested. The study revealed a gradual weakening in the mechanical properties of the soil with increasing FTCs, eventually stabilizing after approximately 10 cycles. This decline in strength was attributed to the diminishing inter-particle bonding. Notably, the elastic modulus, peak friction angle, and cohesion experienced significant reductions of 54 %, 71 %, and 20 %, respectively. This decrease was in the form of rapid weakening in the first cycles and relative stability in the continuation of FTCs.

To mitigate the adverse effect of FTCs on soil strength, several soil improvement methods have been proposed in the literature.

Traditional soil stabilization such as adding lime and cement are categorized as effective but environmentally unfavorable methods. (Nguyen et al., 2019) investigated the effect of fine-grained soil improvement with lime against FTCs. Three types of soils, including silty, low-plasticity clay, and high-plasticity clay, were examined in their study. Adding 4 % and 7 % lime showed the most significant increase in the compressive strength of the samples. Additionally, the effect of lime increased with the prolongation of the curing time. As another example, Aldaood et al. (2021) investigated the impact of enhancing gypseous soil with lime and polypropylene fibers on its strength response to FTCs. The experiments were conducted under two conditions: an open system with water uptake and a closed system without water uptake during FTCs. The findings revealed that specimens subjected to open-FT conditions exhibited a greater decline in resistance compared to those in closed-FT conditions. Since the soils analyzed in (Aldaood et al., 2021)'s study contained gypsum, the quantity of lime necessary to enhance their resistance against FTCs varied depending on their gypsum content.

Zhu et al. (2023) investigated the performance of a clay soil reinforced with polyethylene terephthalate against FTCs. The tested clay was of expansive nature. The behavior of samples in a certain number of FTCs was investigated using repeated load triaxial and unconfined compressive strength tests. It was shown that the compressive strength and resilient modulus of the samples improved by adding 1 % Polyethylene terephthalate strip reinforcement. This improvement was due to the reduction in the development of cracks during FTCs by polyethylene terephthalate reinforcement. (Yang et al., 2024) investigated the effect of adding anionic polyacrylamide (APAM) on increasing the resistance of a silty clay soil subjected to FTCs. To study the effects of adding APAM in different percentages to the soil, zeta potential, thermal conductivity, hydraulic conductivity, and triaxial compressive strength were evaluated. All unmodified samples showed the greatest decrease in the peak shear strength and increase in hydraulic conductivity in the first three cycles of FT. These parameters gradually reached a stable and relatively constant state by increasing the number of FTCs up to 9. The cohesion of modified and unmodified soils decreased with the increase in the number of FTCs. The cohesion of the samples showed the most significant decrease in the initial cycles of FT. With the increase in the number of FTCs, the value of surface porosity, defined as the ratio of pore area to the total area in the SEM image, increases for both unmodified and modified soils. However, the soil with 0.3 % APAM showed the lowest porosity and the lowest frost heave in the freezing phase of the sample. In addition, (Yang et al., 2024) presented an exponential decay relationship for the decreasing trend of cohesion of modified and unmodified soils. However, the decrease in friction angle and failure shear stress observed in triaxial tests up to 9 FTCs still had a decreasing trend and did not reach a stable state.

Bozyigit et al. (2023) investigated the effect of adding eco-friendly polymers to kaolin soil on its strength behavior against FTCs. Different types of polymers such as xanthan gum, guar gum, and anionic polyacrylamide polymer (PAM) were used for soil stabilization. It was shown that the type and amount of polymer and curing time affect the strength of the samples. The increase in unconfined compressive strength (UCS) with the addition of guar gum showed the highest value. There was an increase in strength with increasing curing time in samples stabilized with guar gum and xanthan gum, while this was not the case for samples stabilized with PAM. The effect of PAM on improving performance against FTCs was more than that of guar gum and xanthan gum. Changizi et al. (2022) performed laboratory tests to comprehend how various FTCs might affect clay treated with varied concentrations of nano-SiO_2. The results demonstrated that nano-SiO_2 enhances clay strength. After nine FTCs, the UCS and shear strength of clay treated with 1.0 % nano-SiO_2 were, respectively, 16 % and 21 % higher than those of untreated natural clay, which was not subjected to the FTCs. The SEM images confirmed the alterations in clay mineral arrangement caused by FTCs. From nine to twelve FTCs, however, there was a minimal loss in soil strength. In other words, nine FTCs were enough for the soil structure to reach a stable state.

In addition to the above-mentioned ground improvement methods for modifying problematic soils exposed to FTCs, a sustainable alternative to conventional chemically induced methods, such as adding portland cement, polymers, or other additives to the soil, is the Microbially Induced Calcite Precipitation (MICP) approach. In this method, calcium carbonate $CaCO_3$ is precipitated through a biological reaction catalyzed by a urease enzyme produced by bacteria (DeJong et al., 2010; Assadi-Langroudi et al., 2022). (Rahman et al., 2020) reported details of MICP method in an extensive review. This method has great promise in a variety of applications such as ground improvement to reduce susceptibility against frost action (Xiao et al., 2020). (Sun et al., 2021) studied freez-thaw durability of a loess soil using MICP method. Gowthaman et al. (2020) performed a series of experiments on slope soil exposed to FTCs to evaluate the influence of MICP. Their results illustrated that slope soil improved by the MICP method had good durability against erosion caused by FTCs. The precipitation of $CaCO_3$ between the soil particles increases failure strength, leading to an increase in internal friction and cohesion.

In another study, Ahenkorah et al. (2023) performed 40 UCS experiments on improved sandy soil. They used MICP and Enzyme Induced Calcite Precipitation (EICP) for the treatment of sand specimens with comparable average calcium carbonate ($CaCO_3$) contents that were subjected to FT cycles. It was shown that after a specific number of FT cycles, the average $CaCO_3$ concentration and their corresponding UCS decreased. Due to the presence of unbounded or weakly bonded $CaCO_3$ within the soil matrix, which was subsequently eliminated during or thawing during FT process, the EICP-treated sand specimens appeared to demonstrate a lower strength to FT cycles than MICP treated specimens. The MICP method is commonly used to improve granular soils, such as sands, but its application in clayey soils has been investigated in only a limited number of studies (Wang et al., 2017a; Tian et al., 2020). Traditionally, MICP compounds are introduced through injection into the soil, but this approach has been replaced in some cases by mixing the compounds directly with the soil as an alternative method. However, studies have shown that MICP alone is not highly effective in clays with a high degree of saturation (Ghalandarzadeh et al., 2024; Jiang et al., 2017). To address this limitation, (Ghalandarzadeh et al., 2024)

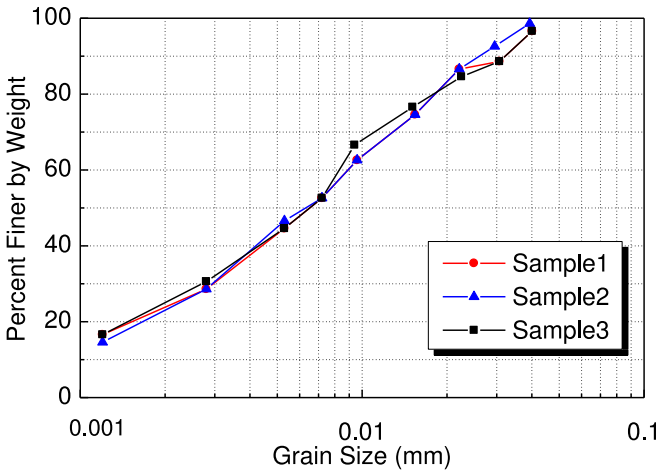

Fig. 1. Grain size distribution curves of the kaolinite samples.

proposed the incorporation of nano-SiO_2 to enhance its effectiveness.

As mentioned above, the MICP process faces limitations in fine-grained soils due to their low permeability and small pore sizes, which hinder the formation and distribution of calcium carbonate precipitates. To overcome these challenges, the incorporation of additives such as nano-silica is necessary. Nano-silica, due to its hydrophilic properties and high surface area, provides nucleation sites, enhances calcium carbonate precipitation, and helps reduce water content in saturated soils. This creates additional space for $CaCO_3$ deposition, improving the mechanical properties of the treated soil. For instance, Ghalandarzadeh et al. (2024) demonstrated that adding 1.5 % nano-SiO_2 to MICP-treated soft clay with 30 % water content significantly improved the unconfined compressive strength (UCS) by enhanced bio-cementation and creating voids for $CaCO_3$ precipitation. Several studies highlight the potential of MICP for improving soil properties when suitable modifications are applied. (Nawarathna et al., 2019) investigated the effect of cationic polysaccharide chitosan on the MICP process. The results confirmed that adding chitosan increased $CaCO_3$ precipitation and strength compared to traditional MICP. Chitosan accelerated the transition from the metastable phase of vaterite to the stable calcite phase, enhancing overall performance. Similarly, Liu et al. (2022) examined the impact of nano-SiO_2 on calcium carbonate precipitation in solution and on quartz grains. While nano-SiO_2 promoted $CaCO_3$ formation in the solution medium. Further emphasizing the potential for improvement, (Zhao et al., 2023) conducted UCS, permeability, and durability tests on sandy soils treated with both MICP and silica powder. The results indicated that silica powder effectively assisted MICP treatment, increasing UCS from 0.41 MPa to 1.12 MPa. Despite these advancements, MICP remains less effective in fine-grained or saturated soils due to limited space for $CaCO_3$ deposition. The use of hydrophilic nano-materials, such as nano-SiO_2, offers a promising solution by absorbing water and creating voids for precipitation, thus enhancing bio-cementation in soils with high water content (Ghalandarzadeh et al. (2024)). The ongoing exploration of additives for MICP demonstrates its adaptability and potential for improving soil stabilization practices.

In regions where FT cycles degrade the strength of clayey soils, there is a growing demand for environmentally sustainable stabilization methods. A key challenge for eco-friendly soil improvement techniques is ensuring their effectiveness in maintaining or enhancing strength under freeze-thaw conditions. This study evaluates the efficacy of a newly introduced nano-bio soil stabilization method in mitigating strength reduction caused by freeze-thaw cycles. To the best of our knowledge, no studies have been done to date to investigate the effect of FTCs on fine-grained soils modified by the nano-SiO_2 enhanced MICP method. A series of triaxial compression tests were conducted to measure the cohesion, shear strength, elastic modulus, friction angle, and stress-strain relations of treated soil samples subject to FTCs.

2. Materials and test methods

2.1. Test materials

Kaolinite clay was chosen as the fine-grained, frost susceptible soil in this study. Three distinct specimens taken from a 20 kg bag were analyzed through hydrometer tests to determine the grain size

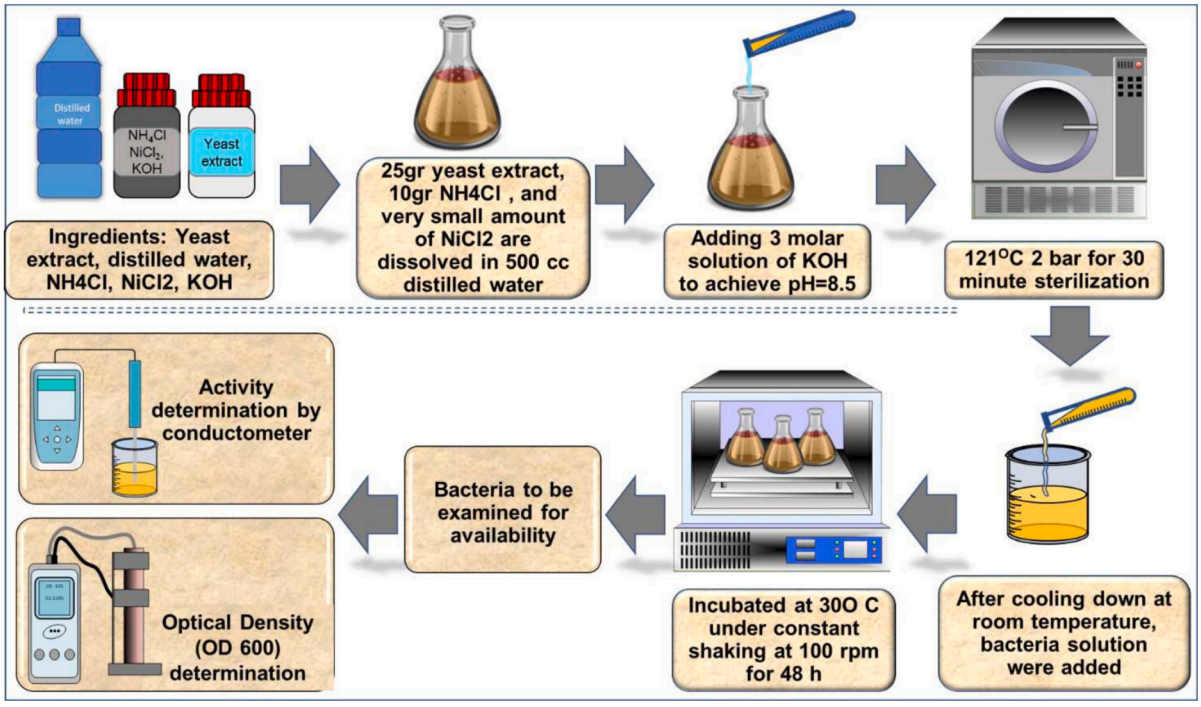

Fig. 2. Cultivation process of bacteria.

Table 1
Physical properties of nano-SiO_2 used in this study.

Mineral Type	Nanoparticle
	SiO_2
Bulk Density	0.10 g/cm^3
Average Particle Size	20–30 nm
Specific Surface Area (SSA)	180–600 m^2/g
Electrical Conductivity	–
Ion Exchange	–
Pore dimension	–
Color	White

distribution, As shown in Fig. 1, the Mean particle size (D50) is about 0.007 mm. The Atterberg limits of the Kaolinite clay samples are as follows: Liquid Limit (LL) of 30.6 %, Plastic Limit (PL) of 19.8 %, and Plasticity Index (PI) of 10.8 %.

2.2. Sample preparation

2.2.1. Preparation of bacteria solution

Bacillus pasteurii, PTCC No. 1645, together with strains from the DSM 33, ATCC 11859, CCM 2056, NCIB 8841, and NCTC 4822, were used in this study. To create the bacterial culture medium, 25 g of yeast extract, 10 g of NH_4Cl, and a small amount of $NiCl_2$ were required to be dissolved in 500 cc of distilled water. For the sterilization process, this solution was placed inside the autoclave for 15 min at 121 °C under 2 bar pressure. The mixture was cooled down at room temperature. For increasing the pH up to 8.5, three molar KOH solution was added to the prepared culture medium. A 5 % by weight of bacteria solution was transferred to the culture medium by a pipette. Finally, the prepared solution was placed inside a shaker incubator at 30 °C at 100 rpm for 48 h. The urea enzyme breaks down urea into ammonium and carbonate ions. This led to an increase in the electrical conductivity of the urea solution. Therefore, the conductivity measurement was used to determine the urease activity of bacteria in the absence of calcium ions. The electrical conductivity was measured using a consort multi-parameter analyzer C 20–30 equipment. Siemens units were used to gauge electrical conductivity. The optical density (OD) for the culture medium and the bacterium solution were 0.44 and 1.12 in turn and the activity of the bacteria solution was greater than 0.5 mS/(cm. min). Fig. 2 shows the cultivation process of bacteria.

2.2.2. Preparation of nano-enhanced bio-treated soil samples

After preparing the bacterial solution, a cementation solution was prepared. 1.1 M solution of calcium chloride and urea was prepared. 360 g of soil was weighed, and 1, 1.5, 2 w.t% of that nano-SiO_2 was added to it, and it was mixed well with a mixer and homogenized. Table 1 lists the physical properties of nano-SiO_2.

The bacteria and cementation solutions were then added to the soil samples in equal amounts and mixed evenly for a couple of minutes. The soil was divided into five layers of 86 g and poured into a cylindrical mold with a diameter of 5 cm and a height of 10 cm, respectively. A tamper compacted each layer with 20 blows. The prepared samples were sealed in vacuum bags and placed in the box for four weeks. The treated and cured samples are designated as MICP30 %-a%NS, where the percentage of MICP solution is 30 %, and the percentage of nano-SiO_2 (NS) is a%. Fig. 3 illustrates the sample preparation process.

2.2.3. Freeze-Thaw cycles

Preliminary experiments were conducted to achieve complete freezing and thawing of pore water in specimens with a diameter of 50 mm and a height of 100 mm, at varying moisture contents. Through a trial-and-error approach, it was determined that maintaining temperatures at −14 °C for freezing and + 14 °C for thawing, each for a duration of 12 h, ensured complete freezing and subsequent thawing of the pore water within the specimens. To confirm this, visual observations were made by breaking the specimens and examining their central parts at different temperatures and durations. This methodology allowed us to establish a protocol to evaluate the performance of the proposed soil improvement method under conditions involving full freeze-thaw cycles.

2.3. Apparatus and test program

This study was intended to investigate the effects of nano-SiO_2-enhanced bio-cementation by MICP on the strength changes of Kaolinite

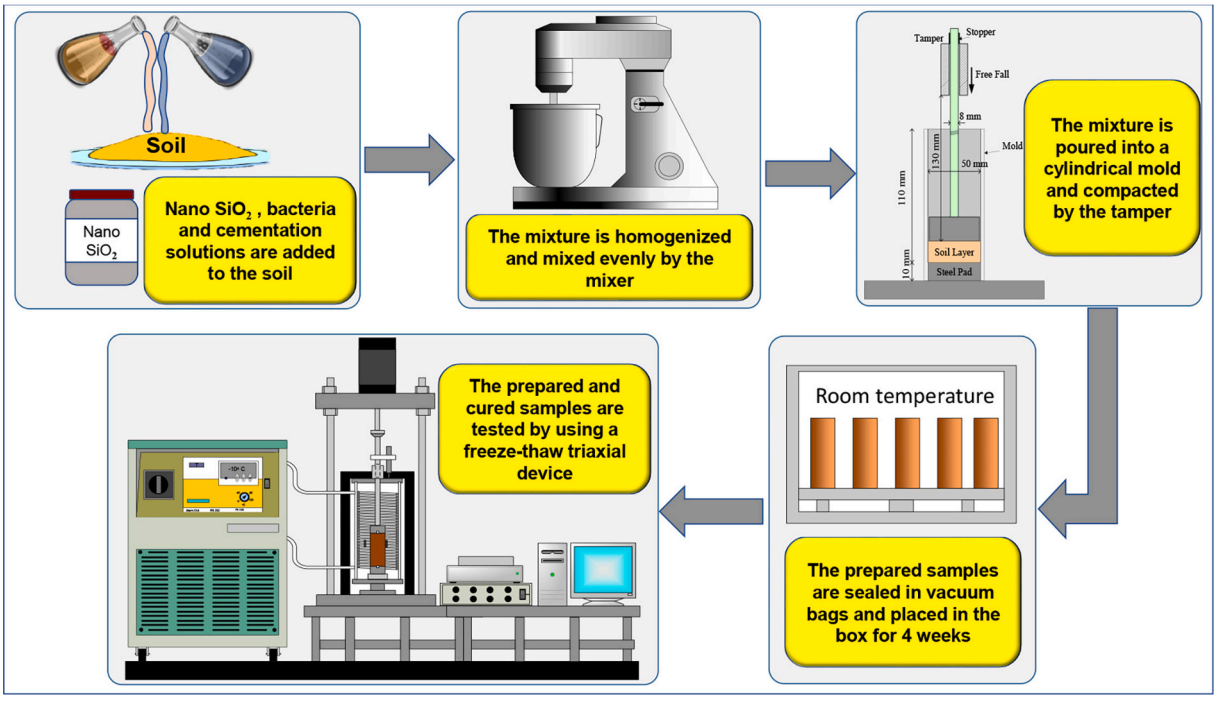

Fig. 3. Sample preparation process.

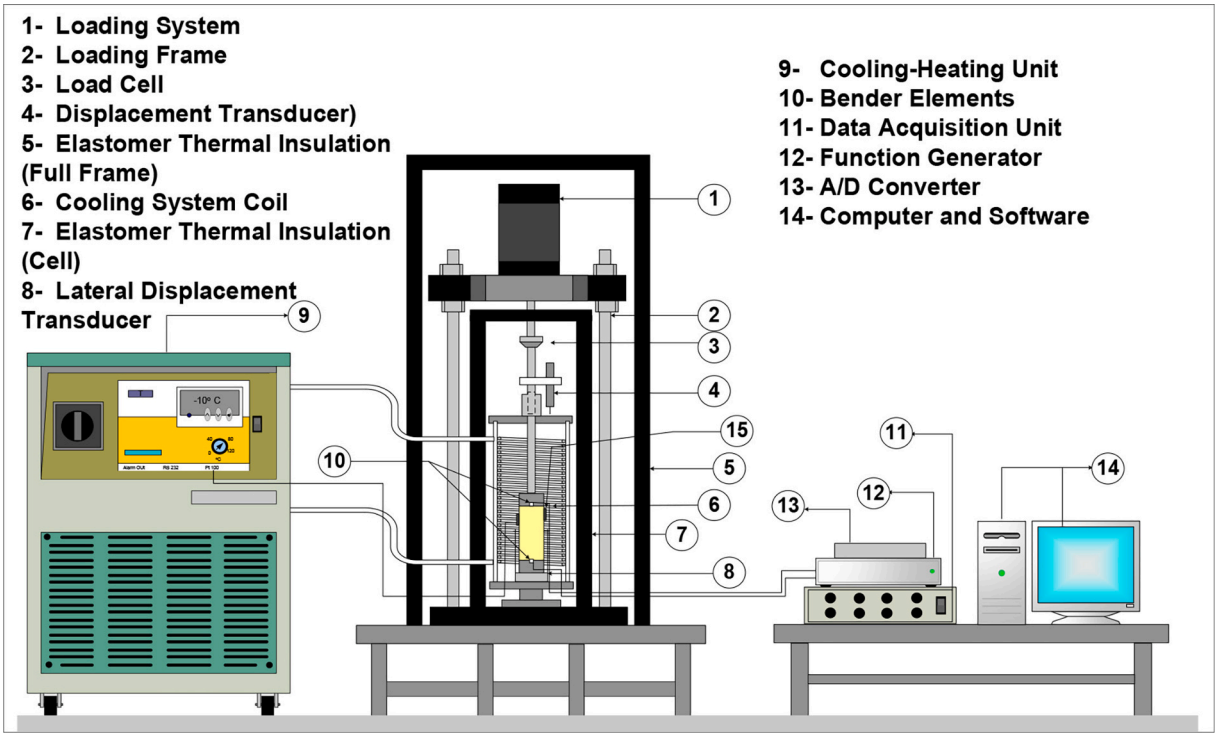

Fig. 4. General layout of F-T triaxial apparatus used in this study.

Fig. 5. Triaxial cell for freeze-thaw tests.

soil subjected to 0 to 6 FTCs. As discussed in the previous section, a triaxial device with the ability to automatically control stress and strain has been set up to perform axial loading tests. An automatic heating-freezing system has also been added to the device to conduct freeze-thaw cycles on in-cell soil samples. Fig. 4 shows general layout of this setup.

Six transducers were used to measure various parameters and apply the necessary controls in the setup: one vertical displacement sensor with 0.01 mm accuracy to measure changes in sample height, one pressure sensor (accuracy of 0.5 kPa) to measure cell pressure, one load cell (accuracy of 1 N) to measure vertical load, and three temperature sensors (accuracy of 0.1 °C) to control and measure in-cell temperature.

Table 2
Test program and the specifications of the performed triaxial tests.

Tested material	FTCs	Temperature (°C)	Confining pressure (kPa)	Number of test
MICP30% NS1%,4 W	0	Tested:+14	50,100,150	3
MICP30%NS1.5 %,4 W	0,2,4,6	Frozen:-14		
		Thawed: +14		
		Tested:+14	50,100,150	12
MICP30%NS2 %,4 W	0	Tested:+14	50,100,150	3
Untreated kaolinite clay	0,2,4,6	Frozen:-14		
		Thawed: +14		
		Tested:+14	50,100,150	12

For triaxial tests, the specimen was first placed in a triaxial cell where cell pressure (50, 100, 150 kPa) was applied (Fig. 5). The temperature control system was then set on −14 °C. The circulation system was activated, cooling the liquid inside the triaxial cell. The control temperature system maintained a constant temperature of −14 °C for 10 h, taking approximately 2 h to reach −14 °C from room temperature. After 12 h, the specimen became entirely frozen. Then the set point was set to +14 °C, which took around 2 h to reach. Following this, the machine maintained a constant temperature of 14 °C for 10 h. After the specimen underwent 2–6 FTCs, a deviator load was applied through a stepper motor-ball screw system that passed through the top of the cell and loaded the sample vertically at a speed of 1 mm/min. The vertical deformation was measured by an LVDT transducer attached to the loading rod, which traveled the same vertical distance as the cap sitting on top of the sample. Moreover, the vertical load was measured by a load cell, placed between the upper cap of the sample and the loading system. Other parameters such as the cell pressure and temperature at the

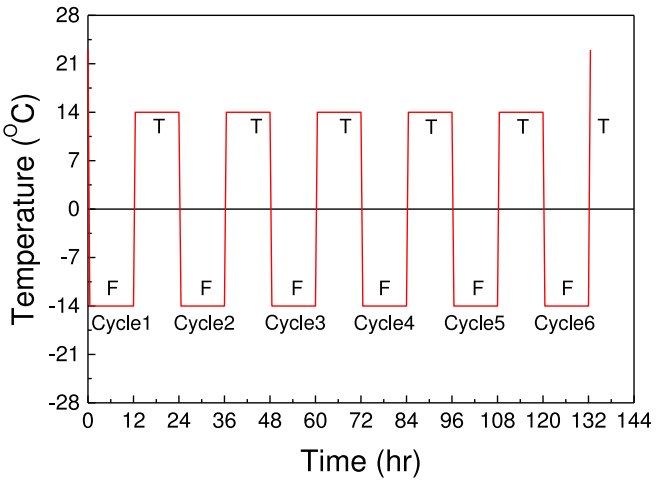

Fig. 6. Schematic diagram of temperature changes and FTCs.

surface of the sample inside the triaxial cell were measured using pt100 temperature transducers. A total of 30 tests were completed on untreated samples with 30 % initial water content and treated samples with 30 % MICP, along with different nano-SiO_2 percentages. Table 2 shows the conducted test program.

The maximum and minimum temperatures were selected as +14 °C and − 14 °C to simulate FTCs to simulate the situation where the entire pore water could be frozen and thaw after 24 h. Fig. 6 shows the temperature cycles during the FTCs. The freezing and thawing process takes 24 h, with each phase lasting 12 h. Most previous studies have typically used a refrigerator to quickly freeze the samples without applying any confining pressure. In this study, a digitally controlled heating-cooling system capable of regulating temperature changes from −47 to +80 °C was used. This system was connected to the triaxial cell to control the temperature inside the cell and allow the FT process to be performed under confining stress. Practically, temperature control inside the triaxial cell was feasible from −25 to +80 °C with an accuracy of ±0.2 °C, while the temperature could be controlled from −47 to +80 °C inside the cooling system reservoir. This system was programmed to apply freeze-thaw cycles within a predefined temperature range. A temperature sensor was connected to the device, close to the heating-cooling copper coil. Another sensor was placed next to the soil specimen inside the triaxial cell to control the temperature at the point closest to the soil specimen. In addition to the PT100 sensor, another temperature sensor inside the heating-cooling reservoir was used for monitoring the entire operation of this system.

As shown in Fig. 7a, the triaxial cell, including all hoses connected to the cell and the heating-cooling system, was covered with an elastomeric thermal insulation coating. The triaxial cell allows the loading rod to be fixed to the top cap of the sample, as shown in Fig. 7b. A copper heating-cooling coil was installed inside this cell. The coil allows the temperature of the cell liquid to be controlled by the heating-cooling system. The size of the copper coil was designed to achieve a stable temperature in the cell liquid and the soil sample. A monoethylene glycol mixture was used as the cell liquid. This mixture can tolerate a temperature range of −50 to 100 °C without freezing or evaporating.

3. Results and discussion

A series of constant strain rate triaxial compression tests on the non-modified and nano-bio modified kaolinite soil samples were completed. Samples were modified with the MICP solution and nano-SiO_2 as an additive to enhance the biocalcification process.

Nano-SiO_2 particles were added at 1 %, 1.5 % and 2 % w.t amount to the soil with 30 % bacteria and cementation solutions with a curing time of 4 weeks. Then, the optimum dosage of nano-SiO_2 was obtained to be tested under FTCs. These tests have been performed on the thawed samples experiencing zero, two, four, six FTCs under 50, 100, and 150 kPa confining pressure levels. Subsequently, the mechanical responses of the soil was evaluated.

3.1. *Investigating the influence of nano-SiO_2-enhanced biocementaton on soil before applying FTCs*

Before the modified and non-modified samples were exposed to FTCs, their strengths were measured with the triaxial UU test based on ASTMD2850-03a. It is important to mention that the tested samples are not fully saturated. Therefore, no pore pressure was measured in the conducted tests. Fig. 8 shows the stress-strain curves of the samples modified with 30 % bacterial and cementation solutions along with 1 % 1.5 %, 2 % nano-SiO_2 under 50,100,150 kPa confining pressure after a curing time of 4 weeks. According to the stress-strain curves, the

(a) External view of the cell covered by an elastomer jacket

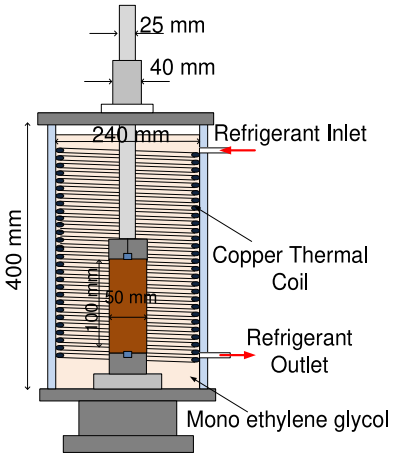

(b) Cross section of the cell and the thermal copper coil

Fig. 7. Triaxial cell.

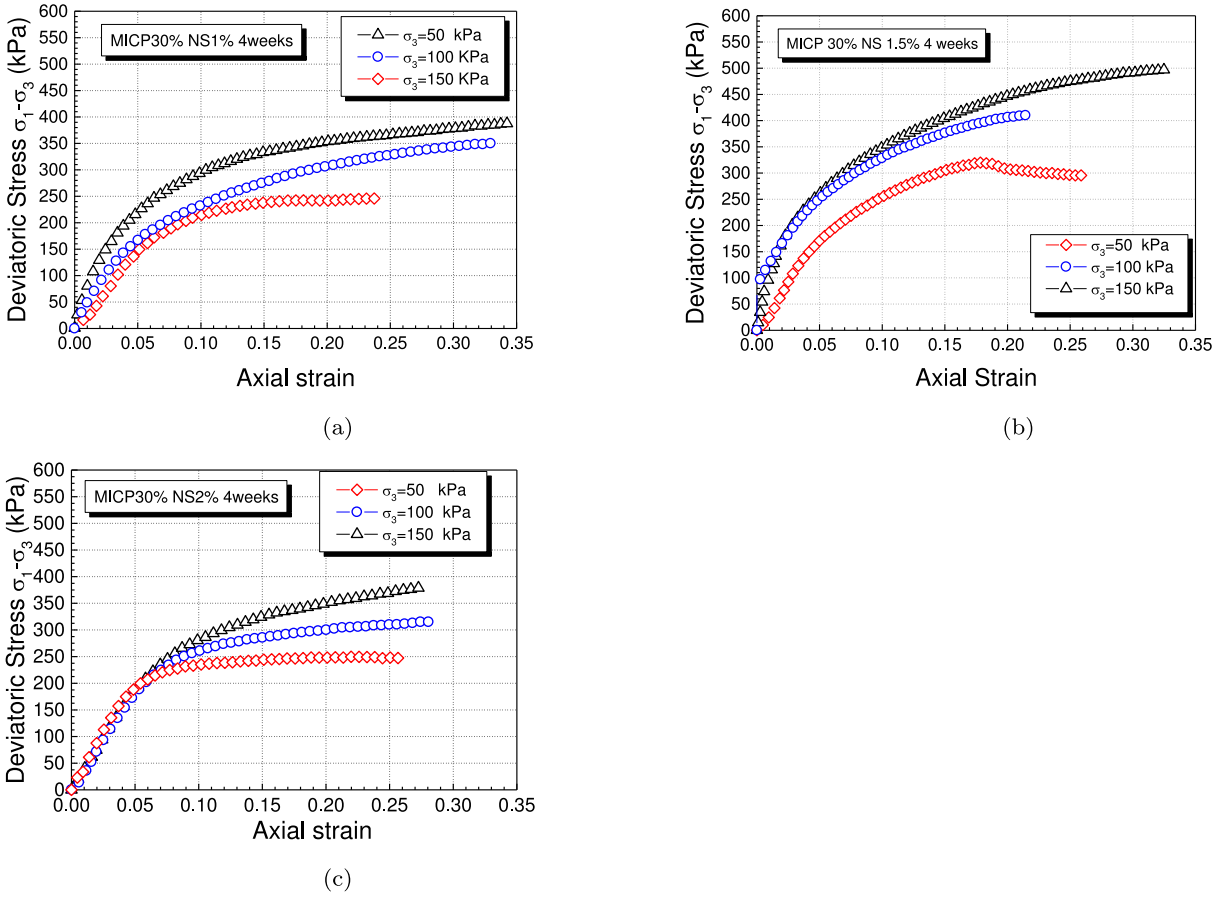

Fig. 8. Results of triaxial test on kaolinite samples treated with 30 % MICP mixed with 1.0 %, 1.5 % and 2 % nano-SiO_2 after 4 weeks curing time before applying FTCs.

deviatoric stress at 20 % axial strain was assumed as the failure strength.

Fig. 9 shows the Mohr-Coulomb failure envelops as well as the effect of different percentages of nano-SiO_2 additives on the cohesion and friction angle of the MICP-treated and untreated samples.

The amount of bacterial solution and cementation is the same in all samples, but nano-SiO_2 varies from 1 to 1.5 % to 2 %. As shown in Fig. 9b, cohesion increases significantly with the addition of nano-SiO_2, but decreases when nano-SiO_2 exceeds 1.5 %. The same trend is observed for fiction in Fig. 9c.

The effect of various percentages of nano-SiO_2 on the Atterberg limits of the soil has also been investigated due to its hydrophilic properties. As shown in Fig. 10a, both the plastic limit (PL) and the liquid limit (LL) increase with an increase in nano-SiO_2 percentage. However, in Fig. 10b, it can be noted that the PL initially declined with the addition of nano-SiO_2 up to 1.5 % and then increases again to 2 %. This suggests that the inclusion of 1.5 % nano-SiO_2 has a more significant effect in lowering the plasticity index of the soil. The increase in cohesion and friction at the presence of 1.5 % nano-SiO_2 corresponds to the minimum plasticity index observed in Fig. 10b.

3.2. Investigating the influence of nano-SiO_2-enhanced biocementaton on soil subject to FTCs

As previously stated, the samples enhanced with 30 % MICP and 1.5 % nano-SiO_2 after 4 weeks of curing time have experienced most improvement in their strength parameters. To examine the performance of the nano-SiO_2-enhanced biocementation treatment on the soil strength, the samples were subject to 2, 4, and 6 FTCs. The samples were exposed to FTCs under a confining pressure of 50, 100, and 150 kPa inside the triaxial cell, respectively. The variation in failure strengths (i.e. the strength at 20 % strain) of untreated and treated samples for different confining pressures and 6 FTCs is shown in Fig. 11. As can be observed, the soil strength decreases as the number of FTCs increases, and this strength reduction is nearly constant after 4 FTCs. This result is in agreement with the observation reported by Tao et al. (2022) where they observed that the resilient modulus and unconfined compressive strength of a cement-fiber treated silty clay soil decreased by increasing freeze-thaw cycles, stabilizing after six freeze-thaw cycles. Due to the sealing of the gaps and fractures that developed during FTCs, the soil strength increases with increasing the confining pressure Wang et al. (2017b).

The failure strength of soil samples after different FTCs is then normalized to the failure strength of the unfrozen sample. The normalized strength can be considered as a reduction factor that shows the strength degradation as FTCs proceeds. Fig. 12 shows the rate of reduction in failure strength as a function of FTCs. As shown, the treated samples had the fastest strength degradation within the first four FTCs. Under the confining pressures of 50 kPa, the maximum reduction was observed. By increasing the confining pressures, it is hypothesized that the rate of reduction decreases and becomes almost the same for larger confining stress levels. After four FTCs pressures the reduction rate almost flattened and a stable state was achieved for all confining pressures.

To investigate the effect of FTCs on the cohesion and friction of the treated samples, their values are plotted versus the number of FTCs in Fig. 13. It can be observed that the degradation rate due to FTCs for cohesion for both treated and untreated samples is more significant compared to that of the friction angle. Although, the cohesion of the treated sample is almost twice the untreated sample at zero FTC, its reduction is faster. This tendency is opposite in terms of the friction

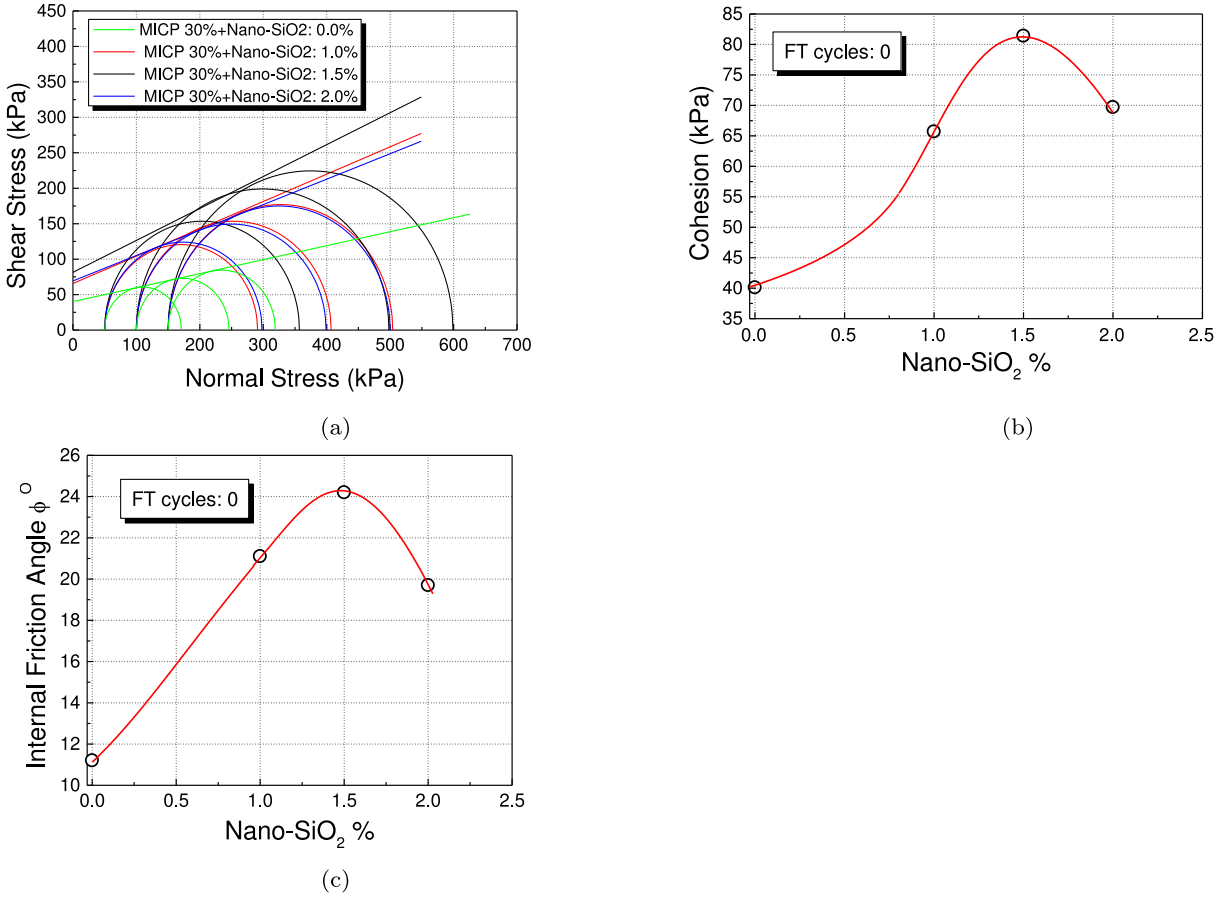

Fig. 9. Comparison of Mohr-Coulomb failure envelops, and cohesion and friction angle of non-modified and 30 % MICP modified samples with 1, 1.5 and 2 % nano-SiO_2.

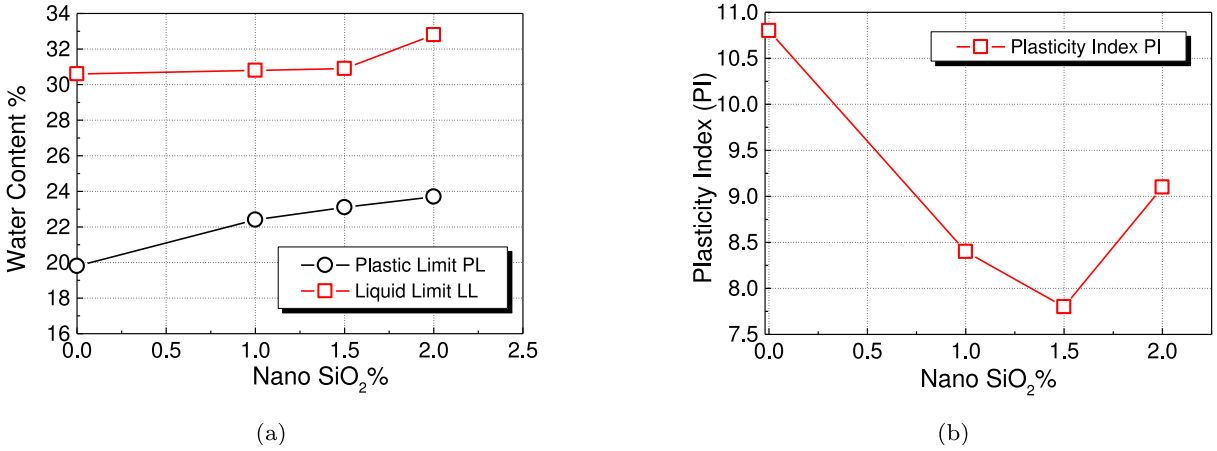

Fig. 10. Effect of nano-SiO_2 on the Atterberg limits and plasticity index of the kaolinite soil samples.

angle. It seems that FTCs has a minor effect on the friction angle of treated samples. However, it is worth noting that, in all FTCs, the treated samples have larger strength parameters compared to the untreated ones. The reduction in cohesion of untreated sample after 6 FTCs is 72 %. Whereas, this reduction is 59 % for treated samples after 6 FTCs.

An empirical formula is presented to fit the experimental data of Fig. 14 for the degradation rate of failure strength for treated samples subject to FTCs, as follows:

$$RF = (1 - RF_{min}) + e^{-(FT^2/D)} \quad (1)$$

where RF is the strength reduction factor, RF_{min} is the minimum stable state strength reduction factor, and D denotes the decay parameter. The decay parameter (D) represents the number of FTCs at which the strength stabilizes at its minimum value. This indicates that further increases in FTCs will not result in a reduction in strength.

As discussed above, a rapid drop in failure strength was observed until the first three FTCs. However, after the third FTC, the rate of strength reduction was slow and it reached a stable state after 4 FTCs. The fitted parameters, as presented in Table 3, are used to plot the failure strength curves based on eq. 1 as shown in Fig. 14.

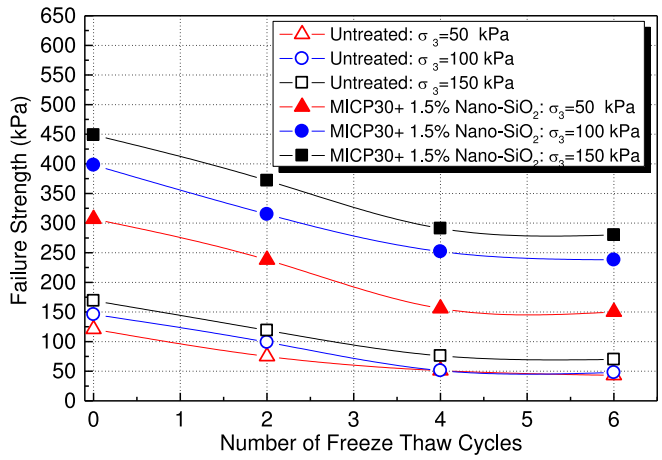

Fig. 11. Effect of FTCs on failure strength of untreated kaolinite treated by 30 % MICP and 1.5 % nano-SiO_2 under different confining stresses.

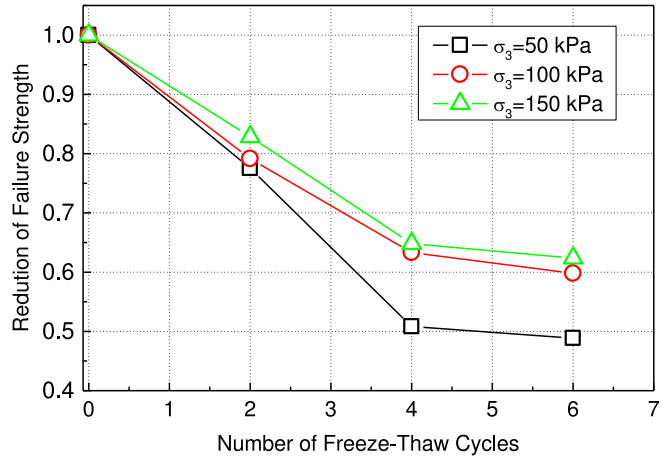

Fig. 12. Effect of FTCs on the degradation of failure strength at 50, 100 and 150 kPa confining pressure.

3.3. *Investigating the influence of nano-SiO_2-enhanced biocementaton on resilient modulus*

The resilient modulus of soils is one of the most important mechanical properties in transportation geotechnics. The resilient modulus can be calculated using the initial tangent stress-strain curve for an axial deformation of 1 % (Kumar and Singh, 2008; Roustaei et al., 2015), as follows:

$$M_r = \frac{\Delta\sigma}{\Delta\varepsilon} = \frac{\sigma_1 - \sigma_0}{\varepsilon_1 - \varepsilon_0} \quad (2)$$

where σ_1 and σ_0 are the deviatoric stresses corresponding to the axial strain $\grave{o}_1$ and $\grave{o}_0$, respectively. Extensive laboratory studies have been carried out to analyze the various factors that contribute to the resilient properties of soils. The resilient modulus can significantly decrease by even a few FTCs (Simonsen et al., 2002).

Fig. 15 shows the changes in resilient modulus for various confining pressures and different FTCs. As the number of FTCs increases, the resilient modulus showes a linear declining trend until 4 FTCs. For unmodified soil samples, the resilient modulus was dropped by 27 %, 57 % and 72 % after 2, 4, and 6 FTCs at 50 kPa confining pressure. However,

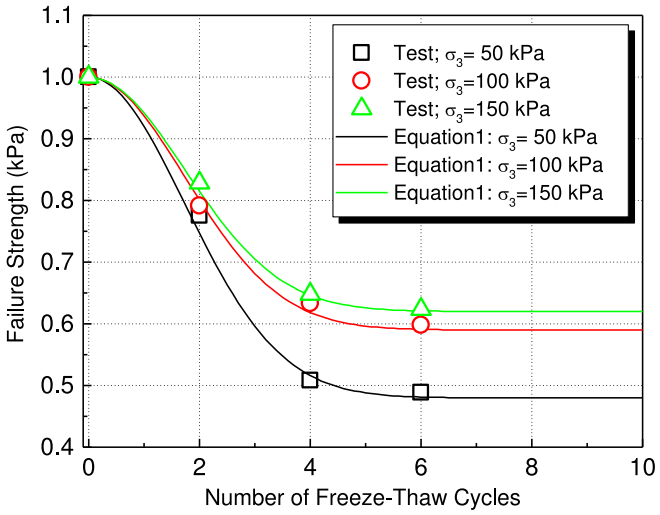

Fig. 14. Comparison of the experimental data and the curves obtained by Eq. 1.

Table 3
The fitted parameters in Eq. 1.

Confining stress (σ_3) (kPa)	RF_{min}	D	R^2
50	0.52	6	o.996
100	0.41	6.5	0.996
150	0.31	7.5	0.997

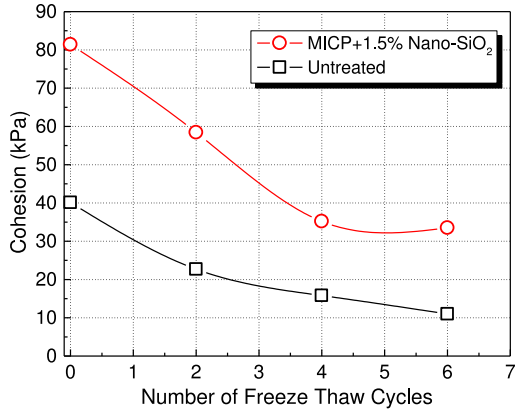

(a)

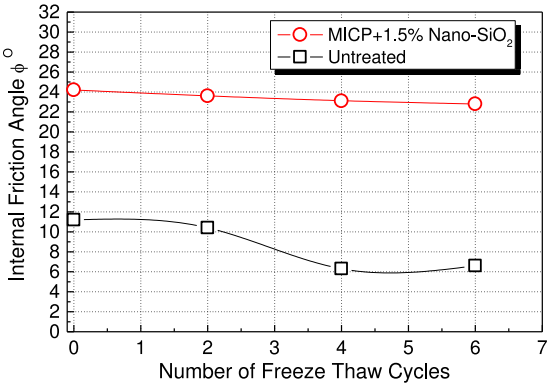

(b)

Fig. 13. Effect of FTCs on cohesion and friction angle of non-modified and modified soil samples.

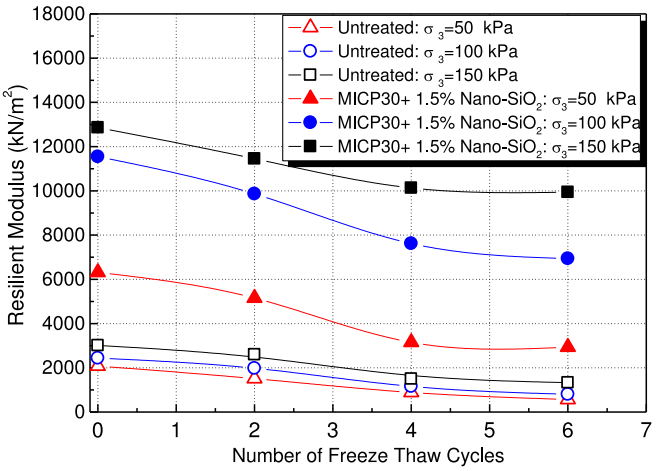

Fig. 15. Effect of FTCs on resilient modulus of non-modified and modified soil at different confining stresses.

for the samples subjected to higher confining pressures of 100 kPa and 150 kPa, this declining trend is less pronounced. After 2, 4, and 6 FTCs, the resilient modulus degradation for a confining pressure of 100 kPa were 18 %, 52 % and 67 %, respectively. The corresponding resilient modulus drop for the 150 kPa confining pressure was 14 %, 50 % and 56 % after 2, 4, and 6 FTCs, respectively.

Similarly, the resilient modulus of treated samples under different confining pressures and FTCs was also assessed. Compared to the untreated samples, the treated samples showed a less degradation in the resilient modulus with increasing in FTCs. The resilient modulus of the modified samples dropped by 19 %, 50 % and 53 % after 2, 4 and 6 FTCs, respectively, all at a low confining pressure of 50 kPa. After 2, 4, and 6 FTCs, for a confining pressure of 100 kPa, the resilient modulus degradations were 11 %, 34 % and 39 %, respectively. For a confining pressure of 150 kPa, the corresponding resilient modulus drops were 10 %, 21 % and 23 %, after 2, 4, and 6 FTCs, respectively. In comparison to the untreated samples, the resilient modulus of the modified samples performed better with increasing FTCs.

3.4. SEM Imaging

To investigate the effect of the employed improvement method at the microscale, a series of Scanning Electron Microscope (SEM) images were taken from the modified soil samples. As shown in Figs. 16 and 17, the distributed colonies of calcium carbonates have created denser and flocculated textures in the sample modified with 30 % bacteria and

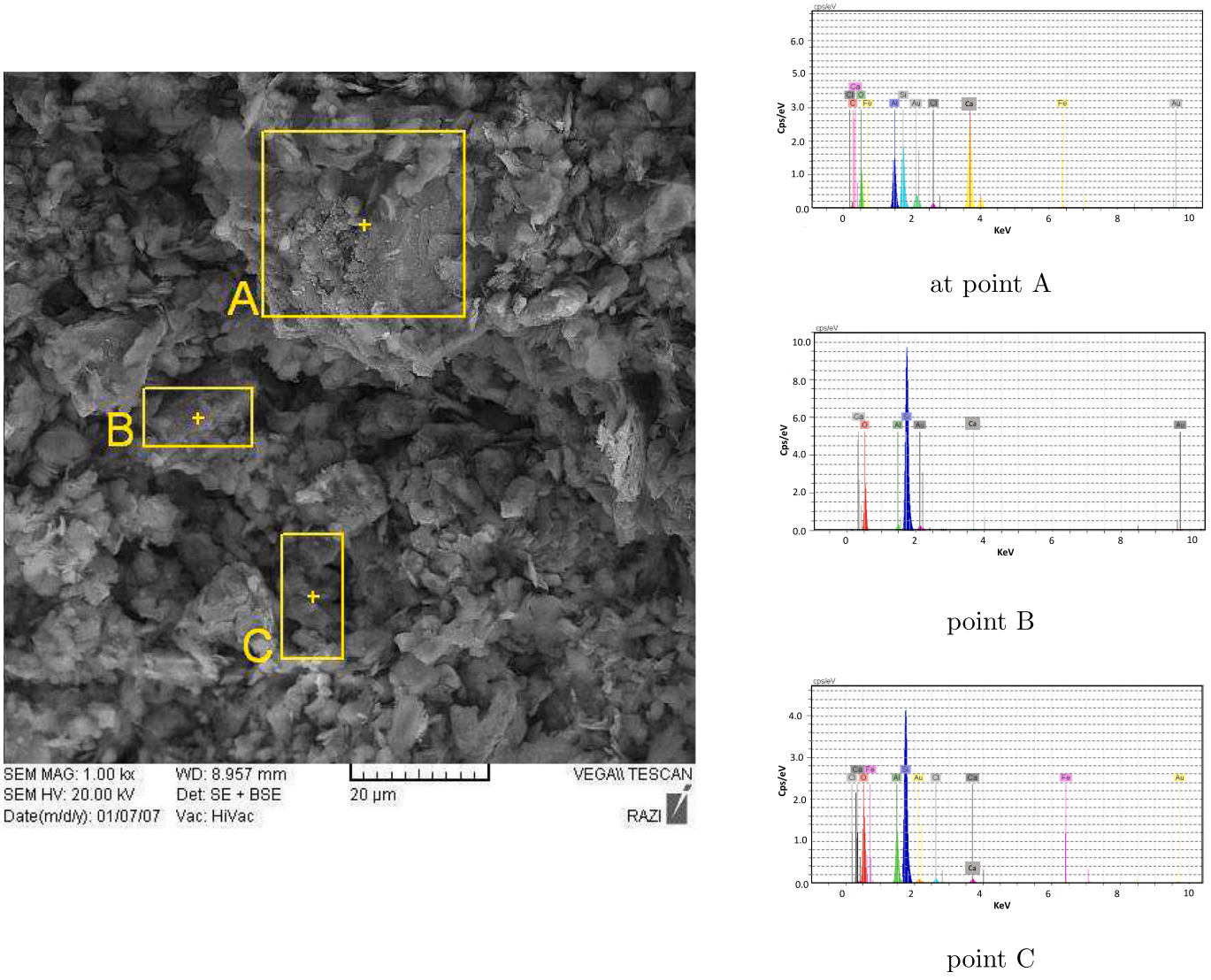

Fig. 16. Scanning Electron Microscope images of sample MICP-30-NS-1.5 and the corresponding Energy Dispersive Spectra at points A, B, and C.

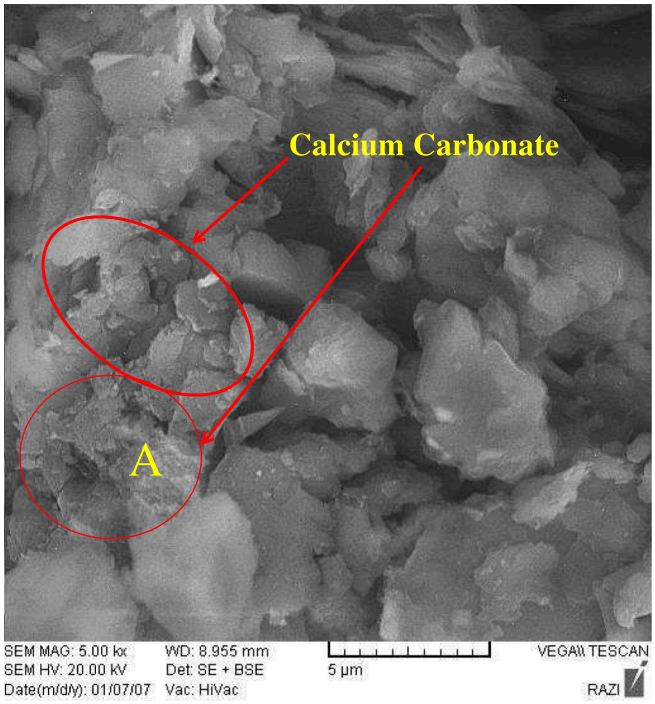

Fig. 17. Scanning Electron Microscope images of sample treated with 30 % MICP solutions and 1.5 % nano-SiO_2; clear difference between clay minerals and agglomerated part.

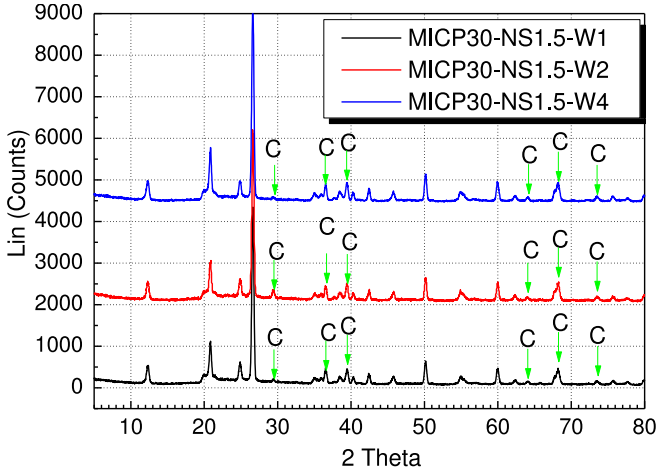

Fig. 18. X-Ray Diffraction of the sample modified by 30 % bacterial and cementation solutions and 1.5 % nano-SiO_2 after W1, W2 and W4 of curing time.

cementation solutions mixed with 1.5 % nano-SiO_2. Colonies of agglomerated calcium carbonate are also seen in Fig. 17. Integrated particles adhered to the clay minerals shows the formation of precipitation of calcium carbonate. It seems that this texture contributed to a stronger bonding between particles that improving the soil behavior under FTCs. Energy Dispersive Spectroscopy of three points A, B and C in the SEM image is presented in Fig. 16. At point A, which belongs to an agglomerated part of the image, abondance of calcium, as shown in the Energy dispersive spetrum, may suggest the presence of calcite that in turn is the product of bio-nano treatment. The absence of calcium can be observed in the Energy dispersive spetrum of the other points of B and C.

The XRD analyses of the samples modified with 30 % bacterial and cementation solutions with 1.5 % nano-SiO_2 after 1, 2 and 4 weeks of curing time is shown in Fig. 18. The main detected components are silicon oxide SiO_2 (Si), kaolinite (K) and calcite (C). As can be seen, calcite peaks are smaller and weaker than other peaks, indicating a lower percentage of its presence in the treated soil after different weeks of curing time.

As can also be seen in Fig. 18, the height of the peaks has slightly increased with increasing curing time.

3.5. *Effect of nano-SiO_2 on enhancing MICP efficiency*

To examine the impact of nano-SiO_2 on improving the strength parameters in MICP-treated samples, its effect on reducing moisture content and plasticity index was first evaluated. The hydrophilic property of nano-SiO_2 leads to water absorption, which helps maintain an optimal free water content for the MICP process, thereby enhancing calcification (Ghalandarzadeh et al., 2024). To investigate the mechanism of nano-SiO_2's effect, SEM images of untreated samples, MICP only-treated samples, and MICP-treated samples with 1.5 % nano-SiO_2 were compared. As shown in Fig. 19a, the untreated sample features discrete sheets of kaolinite minerals without any considerable aggregation or cohesion. However, in the sample treated with MICP, the clusters and aggregates are visibly apparent in Fig. 19b indication the creation of bonded texture. Although these aggregates can be observed in various parts of the sample, their size is smaller and exhibits less cohesion compared to the agglomerated colonies formed in the sample treated with MICP+1.5 % nano-SiO_2. As seen in Fig. 19c, a larger volume of clay and calcite colonies has formed in the sample treated with MICP+1.5 % nano-SiO_2. In addition to its effect on moisture content, it is hypothesized that the nano-SiO_2 particles act as distributed nucleation sites within the soil matrix, leading to the formation of larger calcite precipitate fragments. The increased abundance of agglomerated colonies of clay minerals and calcite induced by the presence of nano-SiO_2 contributes to enhanced cohesion and even an improvement in the soil's internal friction angle, thereby improving its resistance to freeze-thaw (FT) cycles.

Fig. 20a and b present the energy dispersive spectra (EDS) of point A in Fig. 19a, and c, corresponding to the MICP-only and MICP+1.5 % nano-SiO_2 samples, respectively. The calcium peak in the EDS spectrum for the MICP-only sample at point A (the agglomerated region) is significantly shorter (lower) than the corresponding peak for the sample treated with MICP+1.5 % nano-SiO_2. The weight percentages of different elements for the two aforementioned regions are shown in Tables 4 and 5 for the MICP-only and MICP+1.5 % nano-SiO_2 samples, respectively. As observed, the weight percentage of calcium in the sample with 1.5 % nano-SiO_2 is approximately twice that of the sample without nano-SiO_2. This difference indicates that the presence of nano-SiO_2 effectively increases calcium content, which is indicative of higher calcite precipitation. This explains the improved strength parameters and deformation characteristics of the sample treated with the MICP +1.5 % nano-SiO_2 combination.

4. Conclusion

This paper presents the results of a series of experimental studies to evaluate the effectiveness of the nano-bio cementation improvement method, which involves the combined use of MICP and nano-SiO_2, under FT cycles. The addition of nano-SiO_2 aimed to enhance the efficiency of the MICP method in improving the strength of kaolinite soil with a high degree of saturation. The kaolinite soil was treated using a combination of MICP and nano-SiO_2 through a mixing process followed by compaction.

The results of triaxial tests on the treated soil samples revealed that the optimal nano-SiO_2 content is 1.5 %. Consequently, triaxial tests on samples subjected to freeze-thaw cycles were conducted exclusively on samples treated with a combination of 30 % MICP and 1.5 % nano-SiO_2. Additionally, to better understand the performance of the improvement

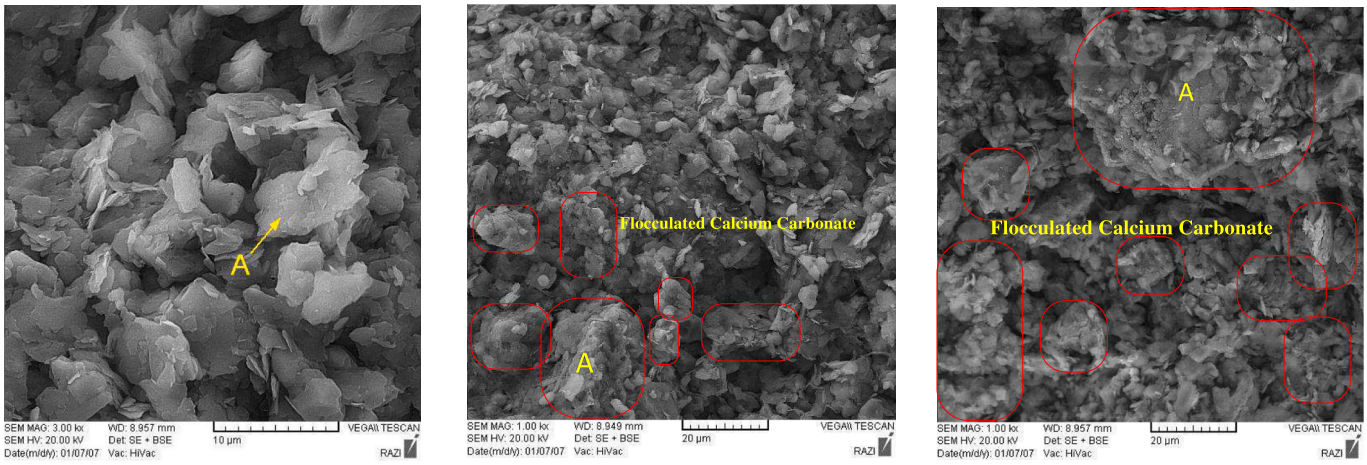

Fig. 19. SEM images of a) untreated sample, b) sample treated by MICP, c) sample treated by MICP+1.5 % nano-SiO_2.

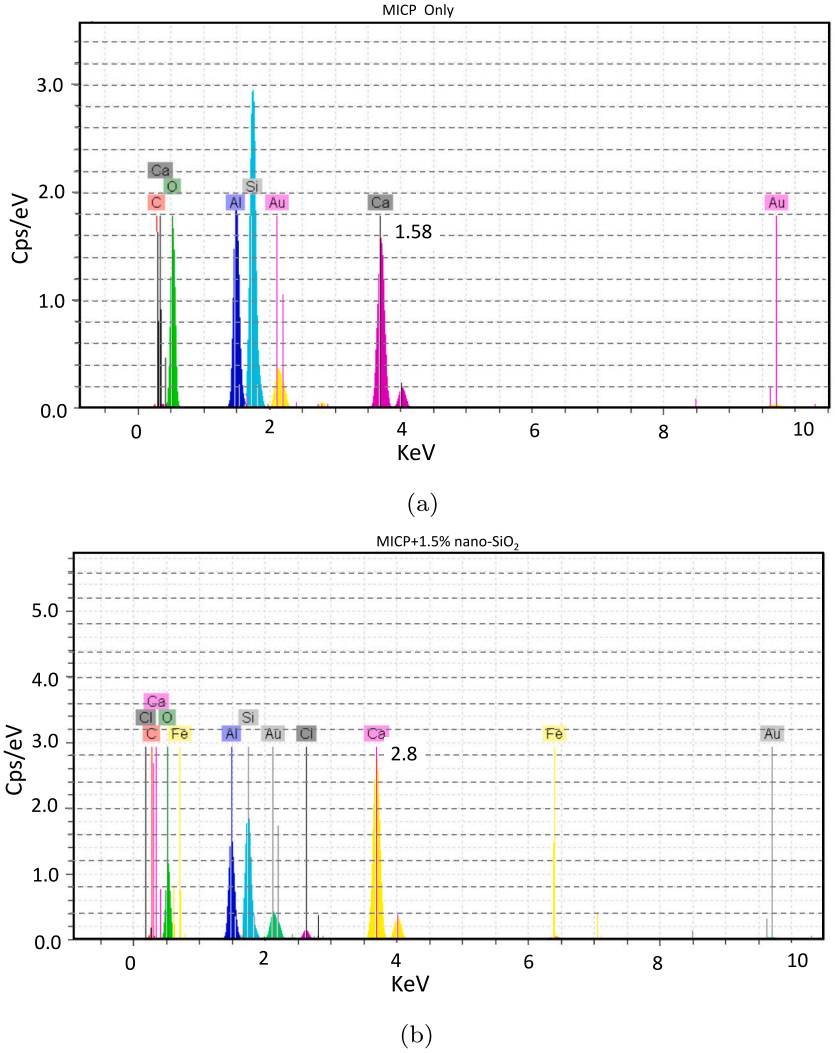

Fig. 20. a) Energy dispersive spectra (EDS) for agglomerated area A of the sample treated by MICP b) for agglomerated area A of the sample treated by MICP+1.5 % nano-SiO_2.

Table 4
Weight percent of different elements reported for energy dispersion spectra (EDS) for the treated sample with only MICP method.

Element	Series	unn. C [wt%]*	norm. C [wt%]**	Atom. C [at.%***
Carbon	K series	1.38	1.63	2.78
Oxygen	K series	47.64	56.49	72.09
Aluminum	K series	8.17	9.69	7.33
Silicon	K series	12.56	14.89	10.83
Calcium	K series	10.76	12.76	6.50
Gold	L series	3.82	4.53	0.47
Total		**84.3 %**		

* *unn. C [wt%]*: The unnormalized concentration in weight percent of the element.
** *norm. C [wt%]*: The normalized concentration in weight percent of the element.
*** *Atom. C [at.%]*: The atomic weight percent.

Table 5
Weight percent of different elements reported for energy dispersion spectra (EDS) for the treated sample with MICP+1.5 % nano-SiO_2.

Element	Series	unn. C [wt%]*	norm. C [wt%]**	Atom. C [at.%]***
Carbon	K series	3.36		6.32
Oxygen	K series	39.07	39.01	55.25
Aluminum	K series	12.54	12.52	10.51
Silicon	K series	15.74	15.71	12.68
Chlorine	K series	1.26	1.26	0.81
Calcium	K series	24.24	24.21	13.69
Iron	K series	0.97	0.97	0.39
Gold	L series	2.97	2.97	0.34
Total		**100.2 %**		

* *unn. C [wt%]*: The unnormalized concentration in weight percent of the element.
** *norm. C [wt%]*: The normalized concentration in weight percent of the element.
*** *Atom. C [at.%]*: The atomic weight percent.

method, X-ray Diffraction (XRD) analysis, Scanning Electron Microscopy (SEM) images, and Energy Dispersive Spectrum (EDS) analyses were performed on the treated samples. The main findings are summarized as follows:

- Before applying FTCs, 1 %, 1.5 % and 2 % nano-SiO_2 were mixed with 30 % bacteria and cementation solutions for 4 weeks curing time. The sample modified with 30 % MICP alonge with 1.5 % nano-SiO_2 had the highest increase in strength compared to the samples with 1 and 2 % nano-SiO_2. Therefore, 1.5 % nano-SiO_2 was chosen as an optimum dosage for enhancing the MICP process. This configuration was applied for investigating the strength of treated samples subject to FTCs.
- FTCs had a significant impact on the strength of the kaolinite clay soil tasted, especially when the confining pressure is low. The strength reduction after 6 FTCs is 51 % for the sample tested under 50 kPa confinement stress, while this reduction is 38 % under 150 kPa.
- FTCs resulted in a reduction in the resilient modulus, failure strength and cohesion. After six FTC, the minimum degradation ranges in treated samples of the failure strength, elastic modulus, and cohesion were 38 % 23 % and 59 %, respectively. In addition, in the untreated samples, the reduction in the failure strength, resilient modulus, and cohesion, after six FTCs, is significantly higher. Therefore, the lower reduction in strength parameters in nano-bio modified sample indicates the successful effect of this modification for soil improvement. In addition to exhibiting less frost-susceptible behavior during freeze-thaw cycles (FTCs), nano-bio treated samples also demonstrated a lower reduction in resilient modulus compared to non-modified soils.
- The application of FTCs resulted in a negligible reduction in friction angle after 4 cycles. Whereas, in the unmodified samples,the friction angle decreased significantly after the 4th FTCs.
- In the triaxial tests, failure strength of specimens decreased with the increasing FTCs and tended to reach a stable value after the 4th cycle.
- The SEM images and XRD analysis clearly show the formation of calcium carbonate colonies and an agglomerated texture in the modified soils. This supports the improvement in mechanical properties of the treated soil samples.
- Increase in cohesion is a result of creation od adhered colonies of clay minerals seen in SEM images. Increase of internal friction is the consequence of formation agglomerated texture of the improved soil. The increase in cohesion is attributed to the formation of calcite colonies adhering to clay minerals, as observed in SEM images. The increase in internal friction results from the development of an agglomerated texture in the treated soil.
- The SEM images of samples treated with MICP only and MICP+1.5 % NS clearly show the formation of agglomerated colonies. However, the larger volume of agglomerated fragments in the samples treated with MICP+1.5 % NS indicates the enhancing effect of nano SiO_2 on MICP stabilization.
- The energy dispersive spectrum (EDS) reveals that the calcium weight percentage in the agglomerated areas of the MICP+1.5 %NS-stabilized samples is significantly higher than in similar areas of the MICP-only treated samples. The presence of nano SiO_2 has led to increased calcification. This can be attributed to its water absorption properties, the creation of greater porosity, and possibly acting as a nucleation site, which promotes enhanced calcite precipitation.

CRediT authorship contribution statement

Sara Ghalandarzadeh: Writing – original draft, Visualization, Validation, Methodology, Investigation, Formal analysis, Data curation, Conceptualization. **Benoit Courcelles:** Writing – review & editing, Supervision, Methodology, Investigation. **Richard Boudreault:** Writing – review & editing, Investigation. **Lukas U. Arenson:** Writing – review & editing, Validation, Investigation. **Pooneh Maghoul:** Writing – review & editing, Validation, Supervision, Resources, Project administration, Methodology, Investigation, Funding acquisition, Formal analysis, Conceptualization.

Declaration of competing interest

The authors declare that they have no known competing financial interests or personal relationships that could have appeared to influence the work reported in this paper.

Acknowledgement

The authors acknowledge the financial support of the Natural Sciences and Engineering Research Council of Canada (NSERC) (ALLRP 576419 - 22) and PRIMA Québec, BGC Engineering Inc., Awn Nanotech, and Object Research Systems.

Data availability

The datasets generated during and/or analyzed during the current study are available from the corresponding author on reasonable request.

References

Ahenkorah, I., Rahman, M., Karim, M., Beecham, S., 2023. Unconfined compressive strength of MICP and EICP treated sands subjected to cycles of wetting-drying, freezing-thawing and elevated temperature: experimental and EPR modelling. Journal of Rock Mechanics and Geotechnical Engineering 15 (5), 1226–1247.

Aldaood, A., Bouasker, M., Al-Mukhtar, M., 2021. Mechanical behavior of gypseous soil treated with lime. Geotech. Geol. Eng. 39, 719–733.
Assadi-Langroudi, A., O'Kelly, B.C., Barreto, D., Cotecchia, F., Dicks, H., Ekinci, A., Garcia, F.E., Harbottle, M., Tagarelli, V., Jefferson, I., et al., 2022. Recent advances in nature-inspired solutions for ground engineering (NiSE). Int. J. Geosynth. Ground Eng. 8 (1), 3.
Bozyigit, I., Zingil, H., Altun, S., 2023. Performance of eco-friendly polymers for soil stabilization and their resistance to freeze-thaw action. Construct. Build Mater. 379, 131133.
Changizi, F., Ghasemzadeh, H., Ahmadi, S., 2022. Evaluation of strength properties of clay treated by nano-SiO2 subjected to freeze–thaw cycles. Road Mater. Pavement Des. 23 (6), 1221–1238.
DeJong, J., Mortensen, B., Martinez, B., Nelson, D., 2010. Bio-mediated soil improvement. Ecol. Eng. 36 (2), 197–210.
Ghalandarzadeh, S., Maghoul, P., Ghalandarzadeh, A., Courcelles, B., 2024. Effect of nanoparticle-enhanced biocementation in kaolinite clay by microbially induced calcium carbonate precipitation. Construct. Build Mater. 414, 134939.
Gowthaman, S., Nakashima, K., Kawasaki, S., 2020. Freeze-thaw durability and shear responses of cemented slope soil treated by microbial induced carbonate precipitation. Soils Found. 60 (4), 840–855.
Jiang, N., Soga, K., Kuo, M., 2017. Microbially induced carbonate precipitation for seepage-induced internal erosion control in sand–clay mixtures. J. Geotech. Geoenviron. Eng. 143 (3), 04016100.
Kumar, P., Singh, S., 2008. Fiber-reinforced fly ash subbases in rural roads. J. Transp. Eng. 134 (4), 171–180.
Liu, M., Cai, L., Luo, H., 2022. Effect of nano-silica on microbiologically induced calcium carbonate precipitation. Construct. Build Mater. 314, 125661.
Nawarathna, T., Nakashima, K., Kawasaki, S., 2019. Chitosan enhances calcium carbonate precipitation and solidification mediated by bacteria. Int. J. Biol. Macromol. 133, 867–874.
Nguyen, T., Cui, Y., Ferber, V., Herrier, G., Ozturk, T., Plier, F., Puiatti, D., Salager, S., Tang, A., 2019. Effect of freeze-thaw cycles on mechanical strength of lime-treated fine-grained soils. Transportation Geotechnics 21, 100281.
Qi, J., Ma, W., Song, C., 2008. Influence of freeze–thaw on engineering properties of a silty soil. Cold Reg. Sci. Technol. 53 (3), 397–404.
Rahman, M., Hora, R., Ahenkorah, I., Beecham, S., Karim, M., Iqbal, A., 2020. State-of-the-art review of microbial-induced calcite precipitation and its sustainability in engineering applications. Sustainability 12 (15), 6281.
Roustaei, M., Eslami, A., Ghazavi, M., 2015. Effects of freeze–thaw cycles on a fiber reinforced fine grained soil in relation to geotechnical parameters. Cold Reg. Sci. Technol. 120, 127–137.
Simonsen, E., Janoo, V., Isacsson, U., 2002. Resilient properties of unbound road materials during seasonal frost conditions. Journal of Cold Regions Engineering 16 (1), 28–50.
Sun, X., Miao, L., Wang, H., Chen, R., Guo, X., 2021. Improvement of characteristics and freeze-thaw durability of solidified loess based on microbially induced carbonate precipitation. Bull. Eng. Geol. Environ. 80, 4957–4966.
Tang, L., Tian, S., Ling, X., Li, G., Zhou, G., 2017. Effect of freeze-thaw cycles on the strength of base course materials used under China's high-speed railway line. J. Cold Reg. Eng. 31 (4), 06017003.
Tao, Z., Zhang, Y., Chen, X., Gu, X., 2022. Effects of freeze-thaw cycles on the mechanical properties of cement-fiber composite treated silty clay. Construct. Build Mater. 316, 125867.
Tian, Z., Tang, X., Xiu, Z., Xue, Z., 2020. Effect of different biological solutions on microbially induced carbonate precipitation and reinforcement of sand. Marine Georesources & Geotechnology 38 (4), 450–460.
Viklander, P., Eigenbrod, D., 2000. Stone movements and permeability changes in till caused by freezing and thawing. Cold Reg. Sci. Technol. 31 (2), 151–162.
Wang, D., Ma, W., Niu, Y., Chang, X., Wen, Z., 2007. Effects of cyclic freezing and thawing on mechanical properties of Qinghai–Tibet clay. Cold Reg. Sci. Technol. 48 (1), 34–43.
Wang, Z., Zhang, N., Cai, G., Jin, Y., Ding, N., Shen, D., 2017a. Review of ground improvement using microbial induced carbonate precipitation (MICP). Marine Georesources & Geotechnology 35 (8), 1135–1146.
Wang, P., Xu, J., Fang, X., Wang, P., 2017b. Energy dissipation and damage evolution analyses for the dynamic compression failure process of red-sandstone after freeze-thaw cycles. Eng. Geol. 221, 104–113.
Wang, M., Meng, S., Sun, Y., Fu, H., 2018. Shear strength of frozen clay under freezing-thawing cycles using triaxial tests. Earthq. Eng. Eng. Vib. 17, 761–769.
Wu, D., Wang, C., Liu, H., Liu, X., 2023. Effect of freeze-thaw cycles on mechanical properties of compacted volcanic ash. Construct. Build Mater. 369, 130637.
Xiao, J., Wei, Y., Cai, H., Wang, Z., Yang, T., Wang, Q., Wu, S., 2020. Microbial-induced carbonate precipitation for strengthening soft clay. Adv. Mater. Sci. Eng. 2020, 1–11.
Yang, J., Li, S., Di, H., Liu, D., Wang, X., Zhao, Y., 2024. Influence of anionic polyacrylamide on the freeze-thaw resistance of silty clay. Cold Reg. Sci. Technol. 219, 104111.
Zhang, A., Zhang, J., Peng, J., Huang, C., Zhou, C., 2022. Effect of freeze-thaw cycles on mechanical properties of an embankment clay: laboratory tests and model evaluations. Frontiers Earth Sci. 10, 865348.
Zhao, Y., Yang, S., Xiao, Z., Zhu, W., Meng, F., Zhang, B., Yuan, M., 2023. Effect of silica powder on microbial-induced carbonate precipitation improvement of medium-coarse sand. Bulletin of Engineering Geology and the Environment 82 (4), 116.
Zhu, J., Saberian, M., Li, J., Maqsood, T., Yang, W., 2023. Performance of clay soil reinforced with PET plastic waste subjected to freeze-thaw cycles for pavement subgrade application. Cold Reg. Sci. Technol. 214, 103957.